LA-UR-97- -3521

Title: ULTRFAST HOLOGRAPHY AND TRANSIENT ABSORPTION SPECTROSCOPY IN CHARGE-TRANSFER POLYMERS

CONF-970706--

Author(s): Duncan Mcbranch and Eric Maniloff
Chemical Science and Technology
Los Alamos National Labortory,
CST-6, MS J567
Los Alamos, NM 87545

Submitted to: SPIE Conference Proceeding, 7/29-8/4/97, San Diego, CA

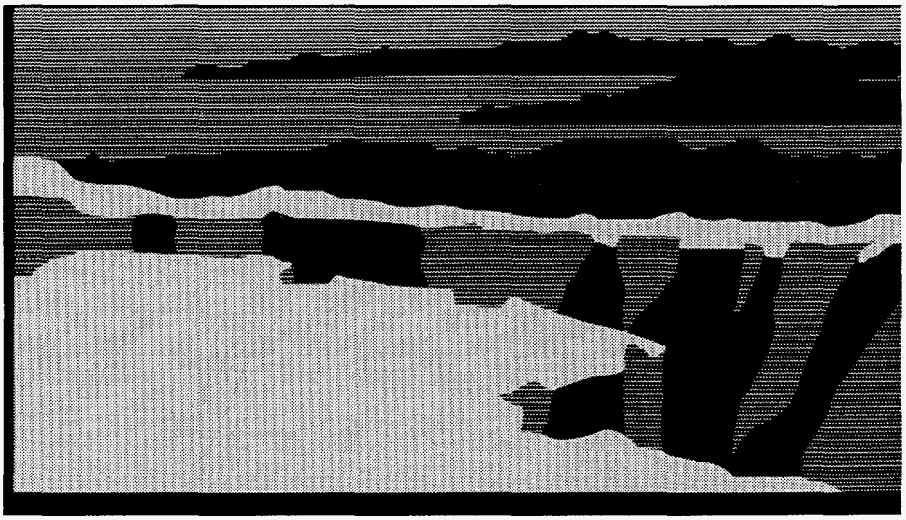

Los Alamos
NATIONAL LABORATORY

Form No. 836 R5
ST 2629 10/91

DISCLAIMER

Ultrafast holography and transient absorption spectroscopy in charge-transfer polymers

Duncan W. McBranch and Eric S. Maniloff

Chemical Science and Technology Division, Mail Stop J567
Los Alamos National Laboratory
Los Alamos, NM 87545

Dan Vacar and Alan J. Heeger

Institute for Polymers and Organic Solids
University of California, Santa Barbara
Santa Barbara, CA 93106

ABSTRACT

Charge-transfer polymers are a new class of nonlinear optical materials which can be used for generating femtosecond holographic gratings. Using semiconducting polymers sensitized with varying concentrations of C_{60}, holographic gratings were recorded by individual ultrafast laser pulses; the diffraction efficiency and time decay of the gratings were measured using non-degenerate four-wave mixing. Using a figure of merit for dynamic data processing, the temporal diffraction efficiency, this new class of materials exhibits between two and 12 orders of magnitude higher response than previous reports. The charge transfer range at polymer/C_{60} interfaces was further studied using transient absorption spectroscopy. The fact that charge-transfer occurs in the picosecond-time scale in bilayer structures (thickness 200 Å) implies that diffusion of localized excitations to the interface is not the dominant mechanism; the charge transfer range is a significant fraction of the film thickness. From analysis of the excited state decay curves, we estimate the charge transfer range to be 80 Å and interpret that range as resulting from quantum delocalization of the photoexcitations.

Key Words: π-conjugated polymers, photoinduced charge transfer, transient absorption, holography

1. INTRODUCTION

Photoinduced charge transfer in conducting polymers leads to charge separation on femtosecond timescales, with back transfer times which can be many orders of magnitude longer.[1] This effect is useful for efficient photoproduction of charge carriers for photovoltaic devices,[2] and for the creation of metastable excited-state populations which lead to enhanced nonlinear optical performance in both holographic information processing[3] and optical limiting.[4] In this paper, we explore the nature of photoinduced charge transfer in blends and bilayers of the conducting polymer poly-(2-methoxy,5-(2'-ethylhexoxy)-1,4-phenylenevinylene) (MEH-PPV, as donor) with C_{60} (as acceptor). We have investigated charge transfer in both disordered bulk blends, as well as charge transfer at the heterojunction formed between thin films of MEH-PPV and C_{60}. We demonstrate the use of charge transfer for generation of ultrafast holographic gratings with tunable time constant and a large enhancement of the time-dependent diffraction efficiency response. The microscopic nature of the charge transfer is then explored in transient absorption dynamics measurements as a function of pump intensity. We estimate the charge transfer range to be 80 Å[5] and interpret that range as resulting from quantum delocalization of the photoexcitations.

Holographic gratings are useful in a variety of dynamical optical applications, including interconnection networks, optical memories, and optical computing.[6] Inorganic photorefractive crystals have been the most widely studied materials for such applications.[7,8] Recently, however, organic holographic materials such as photorefractive polymers, photochromic molecules, and semiconducting polymers, have received considerable attention.[9–11] One of the major problems constraining the practical use of holographic materials has been the trade-off between speed and diffraction efficiency inherent in many classes of materials. The class of materials with the highest diffraction efficiencies has

been photorefractives,[7,12] but the response time has been limited by diffusion (or drift) rates.[13] Third-order ($\chi^{(3)}$) nonlinear optical materials can have essentially instantaneous response times, but have low diffraction efficiencies. In the first part of this paper, we present results of ultrafast holographic recording using C_{60}/conducting polymer blends, and demonstrate that these materials combine the best features of both traditional slow holographic and fast nonlinear optical materials. Charge transfer polymers are demonstrated to exhibit performance two to 12 orders of magnitude better than any previously reported material.

The optical properties of semiconducting polymers are significantly changed with the addition of buckminsterfullerene, C_{60}.[1,14] After photoexcitation across the π–π^* gap, the electron transfers from the polymer (as donor) to the C_{60} (as acceptor). The charge transfer process is ultrafast, ocurring within 300 fs, with a quantum efficiency approaching unity.[15] As a result of the efficient photoinduced intermolecular charge transfer, the photoinduced absorption (PA) and photoinduced reflectance spectral features of the composite films can be significantly enhanced in magnitude over those in either of the component materials.[16] The corresponding changes in the complex refractive index, $\Delta N = \Delta n(\omega) + i\Delta\kappa(\omega)$, imply that charge transfer blends offer promise as nonlinear optical materials; i.e. as holographic materials with absorption gratings in spectral regions where $\Delta\kappa(\omega)$ dominates and as holographic materials with index gratings in spectral regions where $\Delta n(\omega)$ dominates.

To optimize the effect of photoinduced charge transfer for optical signal processing applications, it is first necessary to understand the microscopic nature of the charge transfer process. In turn, this depends greatly on the fundamental nature of the primary photoexcitions in conducting polymers, which remains an important and controversial issue. In particular, to design multilayered devices with length scale optimized for efficient interfacial charge transfer, it is important to know the spatial extent of the primary excitations: is the wavefunction confined to a few repeat units of the conjugated polymer chain, or is it extended over many monomers of the polymer backbone or even extended over multiple chains? Unfortunately, there is not yet a widely accepted answer. Data have been interpreted in terms of models that describe delocalized carriers with small exciton binding energies (0.1-0.2 eV, or less) and spatial delocalization over 30 Å or more.[17] Alternatively, strongly correlated models have been proposed with exciton binding energies from 0.4 eV to greater than 1 eV[18,19] implying primary excitations with wavefunctions localized on the order of a single repeat unit. To resolve this issue, it is important to develop new methods of experimentally determining the spatial extent of excitations in conjugated polymers.

A number of previous experiments have studied the quenching of luminescence in conjugated polymers using nanosecond (ns) time-resolved or CW (non-time-resolved) luminescence measurements, and applied these results to infer a diffusion range for excitons to defects which act as quenching sites. In one class of experiments[20] pristine polymer samples were photo-oxidized in a controlled way to create a variable density of defects on the polymer chains. These defects are formed photochemically in PPV when vinylene linkages are severed to form carbonyl species, which act as electron acceptors and efficient luminescence quenching sites. A diffusion time of order 1 ns was estimated and a corresponding diffusion range of 50 Å was inferred. In a second class of experiments, exciton dissociation properties were inferred from steady-state experiments of bilayer structures comprised of PPV/C_{60},[21] and PPV oligomer/Ca.[22] Dissociation occurs at the interface because the electron and hole are separated by charge transfer. Diffusion ranges of 70 Å and 200 Å, respectively, were inferred.

The C_{60} molecules in the polymer/fullerene mixtures are in some ways analogous to the defect sites in the photo-oxidized polymer system described above.[20,23] With addition of a few per cent C_{60}, luminescence is quenched by approximately three orders of magnitude, relative to the pure conjugated polymer. The implied forward electron transfer rate indicates that charge transfer occurs on the picosecond time scale:

$$\frac{1}{\tau_{CT}} = (\frac{1}{Q})(\frac{1}{\tau_{rad}}) \leq 10^3 \times 10^9 < 10^{12} s^{-1} \quad (1)$$

where $1/\tau_{CT}$ is the charge transfer rate, $1/\tau_{rad}$ is the radiative lifetime, and Q<<1 is the quenching ratio. Measurements of photoinduced absorption and photoinduced dichroism showed that in the polymer/fullerene system charge transfer occurs within a few hundred fs,[24] in agreement with Eq. 1.

The ultrafast charge transfer process has been recently challenged.[25] A forward charge transfer time of more than 10 ps was inferred from transient absorption studies on a heavily doped PPV-derivative/C_{60} blend. In the second part of this paper, we present a detailed study of the intensity-dependent PA dynamics in MEH-PPV/C_{60} blends over a larger range of concentrations, as well as the dynamics of charge transfer at a donor/acceptor interface,

to resolve this controversy. Even in relatively thick bilayer structures, we observe the effects of charge transfer in the picosecond regime. We develop a quantitative model which describes the ultrafast nature of the charge transfer process in MEH-PPV/C_{60} composites and bilayers. The change in dynamics during the first picoseconds results from charge transfer occurring in parallel with exciton-exciton bimolecular recombination. The dynamics of photoinduced charge transfer can be used to infer a spatial extent of the excitons on timescales too short for diffusion to play a significant role. We show that the dynamical data imply a delocalization of the excitonic wavefunction in MEH-PPV over approximately 80 Å. Diffusion across this distance in less than a picosecond is eliminated as a possibility. Delocalization over such distances implies that the exciton binding energy must be relatively small.

2. EXPERIMENTAL

The MEH-PPV/C_{60} blends were spin cast at 1500 r.p.m. to obtain 2000 Å thick films [optical density (OD) = 2 at peak absorption]. Blends having three concentrations of the acceptor molecule were prepared: 5%w (2%M), 10%w (4%M) and 25%w (10%M). Visual examination showed that the films were of excellent optical quality. For bilayers, 200 Å MEH-PPV films (measured with Dektak profilometer) were spin cast at 4000 r.p.m. from dilute solution onto sapphire substrates. The measured OD for the polymer layers was 0.2 at maximum absorption. Subsequently, a 400 Å layer of C_{60} was evaporated onto the MEH-PPV layer.

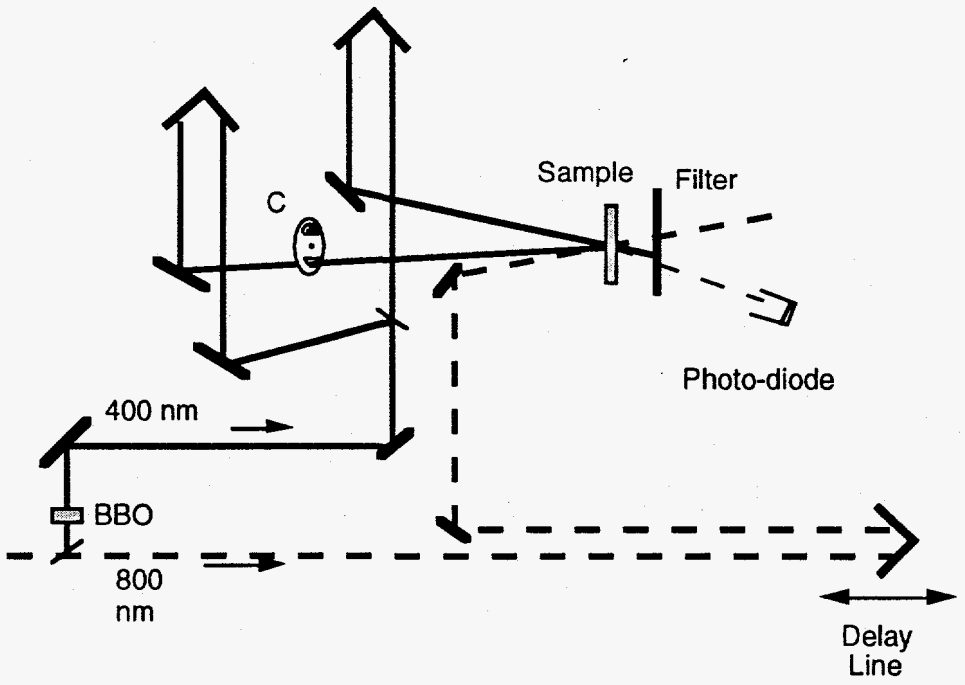

Figure 1. Experimental setup. C=chopper. The 800 nm beam is represented by a dashed line, and the 400 nm beam by a solid line. By delaying the probe (800nm) beam with respect to the pump beams the time dynamics of the recorded grating can be monitored.

A schematic diagram of the nondegenerate four-wave mixing (NDFWM) instrumentation is shown in Fig. 1. The second harmonic of a regeneratively-amplified Ti:sapphire laser (Clark-MXR CPA 1000; pulsewidth $\approx$ 150 fs at the sample plane) operating at 800 nm was split into two beams to generate the holographic grating. The crossing angle of the pump beams was 10 degrees. The gratings were detected using a probe beam at the fundamental wavelength, incident at an angle of 7 degrees as measured from the sample normal. All three incident waves were vertically polarized. Diffracted signal intensities were detected by chopping one of the pump waves at a frequency of 140 Hz, and measuring the diffracted beam using synchronous (lock-in) detection. The probe was time-delayed with respect to the pump by passing the probe beam through a computer controlled delay line before the sample.

This configuration was also used to measure PA at 800 nm by pumping with a single chopped 400 nm beam and detecting modulation in the transmitted probe intensity. At 400 nm, the polymer absorbs strongly, while the

absorption from C_{60} is relatively much smaller. Therefore, the C_{60} molecules are not excited directly by the pump in significant quantity. The pump energy was approximately 3 μJ per pulse illuminating an area of 1 mm^2 at the sample plane. The intensity of the pump beam was varied using neutral density filters. During the measurements on the bilayer structure, the pump and the probe beams were incident on the C_{60} layer and reached the polymer through the C_{60}/polymer interface. The samples were kept in vacuum to avoid photo-oxidation. All measurements were performed at room temperature.

3. HOLOGRAPHIC GRATINGS IN CHARGE TRANSFER BLENDS

Holographic recording using photoinduced charge transfer has a number of characteristics which distinguish it from the large body of materials previously discussed in the literature: 1) The materials respond on a femtosecond timescale, 2) a larger diffraction efficiency is achieved than any previous report using ultrafast materials, and 3) control of the holographic relaxation rate is achieved by use of a two-component recording mechanism. Simply comparing the maximum diffraction efficiency or the response time of different materials does not allow an adequate comparison of their relative merits, since rapid data processing requires having both a large response and a rapid recording rate. As a figure-of-merit to allow comparison with other published work, we therefore define the temporal diffraction efficiency (TDE) as η/τ, with η being the diffraction efficiency and τ being the time constant governing the holographic grating buildup. The TDE gives a measure of how fast and how strongly a material responds to the recording waves, and therefore of how rapidly the material can be expected to be used for data processing. When using this figure of merit, it is important to note the intensity at which the measurement is made as well as the saturation diffraction efficiency, since increasing the recording intensity will affect the rate at which a grating is recorded, and a high value of the TDE does not necessarily imply that a material has a high enough maximum response for a particular application. As an example, photorefractive materials have large efficiencies (approaching unity), but because they respond on times $\geq$ 1s, they have TDE values $\leq 1\ s^{-1}$, for intensities of approximately one W/cm^2.

A large number of materials that undergo photo-isomerization have recently been reported,[26–29] and suggested as possible elements for dynamic holographic processing. The TDE of these materials is in the range of $10^{-1} - 10^{-6} s^{-1}$, with recording intensities typically in the range of 10-50 mW/cm^2. For example, in Ref.[26] the maximum diffraction efficiency reported is 5%, with a recording time constant of 3.2 s for an intensity of 19 mW/cm^2, corresponding to a TDE of 1.6×10^{-2}. An interesting result from studies of photo-isomerization has been that using a NDFWM approach leads to a significant improvement in the diffraction efficiencies.[26] In our studies of charge-transfer holography we adopt this approach, since it is ideally suited to charge-transfer polymers in which new absorption bands are formed after photo-excitation. In addition, we develop a simple model which explains the origin of the enhancement.[3]

Third-order nonlinearities have been extensively used for degenerate four-wave mixing in organics[30,31] and for demonstrations of optical processing.[11] Because of the ultrafast response of these materials, TDE values as high as $10^9\ s^{-1}$ ($\eta \approx 10^{-4}$ in 160 fs) have been reported for pulse energies of ≈ 5 μJ (500 μJ/cm^2). As a mechanism for incoherent third order nonlinearity,[32] $\chi^{(3)}_{inc}$, the photoinduced electron transfer of semiconducting polymer/C_{60} blends offers two important advantages: the metastability of the charge transfer enables control of the grating decay dynamics by varying the concentration of acceptors in the blend, and the photoinduced charge transfer enhances the magnitude of the modulated changes in the complex index of refraction at certain wavelengths. For holographic recording in charge-transfer polymers, we use a pump beam that is strongly absorbed in the host polymer, in order to obtain a large population of photoexcitations. We use a probe wavelength near the peak of the excited state absorption, such that the probe wave is fully transmitted in the absence of the recorded grating, but is strongly diffracted by the recorded grating.

Fig. 2 shows normalized PA data for MEH-PPV blended with varying levels of C_{60}. The data are normalized in order to show the increase in the material relaxation time for increasing C_{60} concentration. The results demonstrate that it is possible to control the relaxation dynamics following photo-excitation by varying the density of electron acceptors.

Fig. 3 shows the temporal dynamics of holographic gratings recorded in the same samples used for generating the PA data in Fig. 2. The maximum diffraction efficiency observed in these experiments was 1.6%, and was observed for the pure MEH-PPV film. The peak diffraction efficiency at 100 fs was reduced by approximately 25% in the sample containing 25% C_{60}, due to the shift in the PA band. Applying the measured spectral dependence of the

CW photoinduced Δn and $\Delta\kappa$ in similar materials, it is clear that by selecting a longer probe wavelength, or using pulsewidths ≥ 1 ps, the nonlinear response of the polymer/C_{60} blend would be enhanced over the neat polymer.[16] *Because of the increased efficiency and ultrafast response, the TDE in our experiments is 10^{11}, two orders of magnitude larger than that reported for other third-order nonlinear polymer experiments, 11 orders of magnitude larger than the best photorefractives, and 12 orders of magnitude larger than results reported using photo-isomerization.*

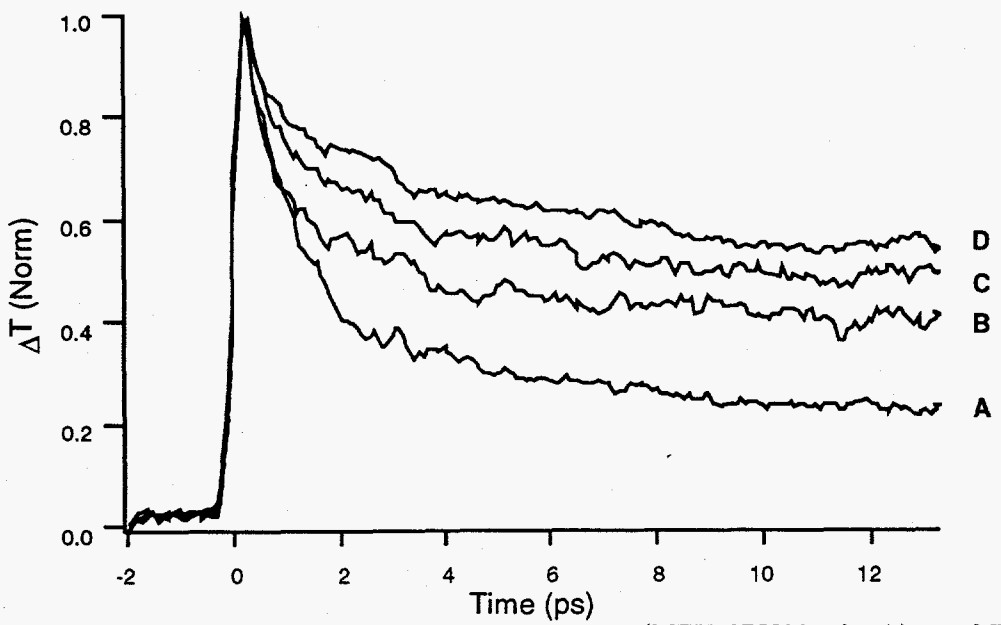

Figure 2. Normalized transient absorption signals observed in C_{60}/MEH-PPV blends. A) pure MEH-PPV B) MEH-PPV with 5% C_{60} C) MEH-PPV with 10% C_{60} D) MEH-PPV with 25% C_{60}.

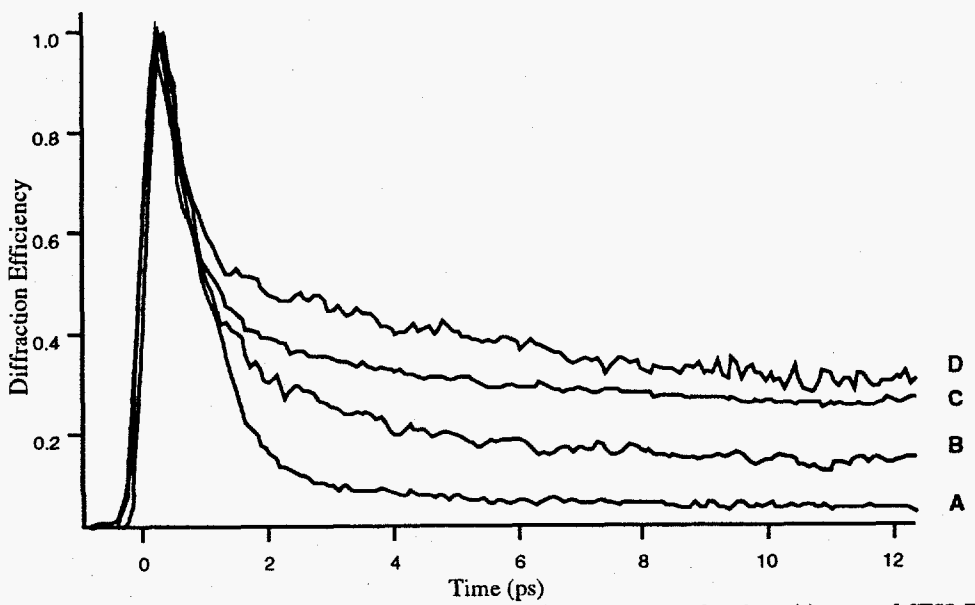

Figure 3. Normalized holographic signals observed in C_{60}/MEH-PPV blends. A) pure MEH-PPV B) MEH-PPV with 5% C_{60} C) MEH-PPV with 10% C_{60} D) MEH-PPV with 25% C_{60}. The maximum diffraction efficiency observed was 1.6%.

Since the holographic diffraction efficiency is proportional to the square of the modulation in ΔN (for small modulations), the square of the decay of the PA signal should match the decay of the diffracted beam.[8] This was observed to be the case (as shown in Fig. 4) only when the PA signal is generated by a pump with the same intensity

as the coherent sum of pump intensities used for forming the transient gratings. As examined in more detail below, the PA decay dynamics are strongly intensity dependent.[33]

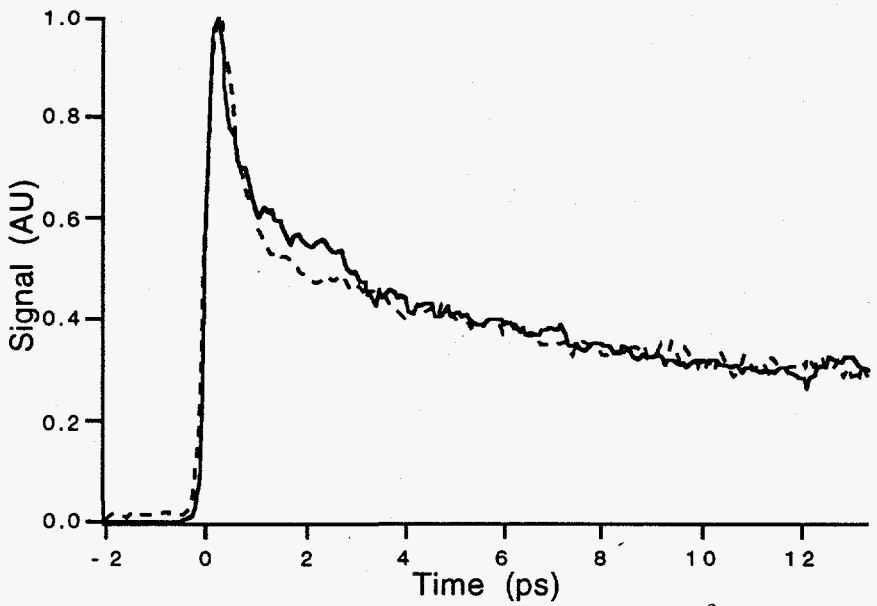

Figure 4. Decay dynamics (normalized) for the square of the PA signal (PA^2, solid line) and the transient grating signal (dashed line) probed at 800 nm. To observe matching dynamics, the same effective pump intensities must be used (see text).

To give insight into the increased diffraction efficiency using nondegenerate as opposed to degenerate four-wave mixing, we use a simple analysis for thin holographic gratings, in which *refractive index* gratings arising from the induced absorption are neglected. We write the ground state population density N_{ex} in the presence of the resonant recording (pump) beam as

$$N(x) = N_0 - N_0\left(\frac{P}{2} + \frac{P}{2}\cos\left(\vec{K}\cdot\vec{x}\right)\right), \tag{2}$$

for the case of a grating with modulation in the x direction, where P is the fraction of the ground state population N_0 which has been depleted ($P = 1$ corresponds to a complete population inversion). In the case of a resonant (degenerate) probe beam, the transmitted amplitude, E_t, is given by:

$$E_t = E_0 \exp\left(-\sigma_g N(x) z\right), \tag{3}$$

where σ_g is the ground-state absorption cross section for the degenerate probe beam and E_0 is the incident wave amplitude. Combining these equations, one can write the diffracted wave, E_d, as

$$E_d = E_0 \frac{\sigma_g N_0 P z}{4} exp\left[-\sigma_g N_0\left(1 - \frac{P}{2}\right) z\right] \tag{4}$$

in the limit of small modulations. This expression contains the magnitude of the modulation of the resonant absorption ($\sigma_g N_0 D$) multiplied by an exponential damping term with the average (large) resonant absorption in the exponent. A similar analysis results in the following expression for the nondegenerate diffracted beam:

$$E_d = E_0 \frac{\sigma_e N_0 P z}{4} \exp\left(-\frac{\sigma_e N_0 P}{2} z\right), \tag{5}$$

where σ_e represents the absorption cross section of the excited state at the probe wavelength. The exponential damping term in this expression is smaller than that in Eq. (4) for $P < 1$. As an example, assuming $P = 0.2$, the maximum diffraction efficiency (η) for the degenerate case is $\eta = 0.042\%$ for $\sigma_g N_0 z = 1.11$. For the same conditions in the nondegenerate case, assuming $\sigma_e = \sigma_g$, $\eta = 0.25\%$. The diffraction efficiency in the nondgenerate case can be

further increased by using a more absorptive (thicker) sample, up to a theoretical maximum of 4.0%. Calculation of this maximum requires including additional terms in the expansion used to derive Eq. 5. Including the effects of photoinduced changes in the index of refraction in the above analysis would lead to further enhancements of the diffraction efficiency in the nondegenerate case.

Eq. 5 indicates that the diffracted wave is proportional to the amplitude of the probe beam E_0 and to the excited-state population N_0P. Since N_0P is proportional to the intensity of the pump beam ($I_p \propto E_p^2$), the diffracted wave can be written as

$$E_d = \chi^{(3)}_{inc} E_p^2 E_0 \tag{6}$$

where $\chi^{(3)}_{inc}$ is the equivalent incoherent third-order susceptibility. Note that since the excited-state population, N_0P, is independent of the pulsewidth (for pulsewidths less than the decay time), $\chi^{(3)}_{inc}$ depends on the fluence, rather than on the flux. To obtain a 1.6% diffraction efficiency from a nonresonant, coherent third-order nonlinearity with the same pump power would require $\chi^{(3)} \geq 10^{-8}$ esu. Thus, $\chi^{(3)}_{inc}$ obtained from the charge transfer blends is 2–3 orders of magnitude larger than nonresonant coherent $\chi^{(3)}$ values typical of conjugated polymers (10^{-11}–10^{-10} esu).[32]

Because this process relies on excited states to produce the hologram, equivalent diffraction efficiencies will be obtained using longer pulses with the same pulse energy provided that the recording pulses are shorter than the ground state recovery time. Charge transfer from the polymer to C_{60} thus allows access to the same diffraction efficiencies with longer pulses (due to the metastability of the excited state). We therefore anticipate that these materials will prove useful over a wide range of pulsewidths, from femtoseconds to microseconds.

4. TRANSIENT ABSORPTION STUDIES OF INTERFACIAL CHARGE TRANSFER

Transient photoinduced absorption data obtained at 800 nm from MEH-PPV/C_{60} bilayers and blends are presented in Fig. 5. The incident excitation density for all data in Fig. 1 was $N_0 = 2.5 \times 10^{19}$cm^{-3}. The population decay in the blends slows down as the acceptor concentration increases from the pure sample to the 25%w blend. The results for the bilayer-structures correspond to the thinnest MEH-PPV film that we could prepare. Two other films produced data that were identical, within the experimental resolution, to the data presented here.

Three experimental facts emerge from Fig. 5: (i) The presence of C_{60} in the vicinity of the polymer (at the interface in bilayers or intermixed in blends) slows down the decay dynamics relative to the decay in the pure samples. As a consequence of the charge transfer, the excited state of the polymer/C_{60} system is longer lived than the excited state of the pristine parent polymer. (ii) The quenching of the fast component decay is evident on subpicosecond timescales, indicating that charge-transfer occurs on the picosecond-time scale in bilayer structures (thickness 200 Å). (iii) The decay dynamics of the polymer/fullerene bilayer system (MEH-PPV thickness 200 Å is essentially identical to the decay dynamics of the 5%w homogeneous blend. Comparison of the blend data in Figs. 2 and 5 reveals that the latter data show substantially slower decay dynamics for the same C_{60} concentrations. This apparent discrepancy arises because the dynamics are strongly intensity-dependent.[33] With these experimental observations in mind, we turn to a discussion of the nature of the excited state and the decay mechanisms that lead to the observed features.

Diffusion of localized excitations to the interface cannot explain the observation of charge transfer in bilayers within the picosecond regime. The diffusion length over a distance d can be expressed as $d^2 = Dt$, where D is the diffusion coefficient and t is the time. Assuming $d = 100$Å for the bilayers and $t = 10^{-12}$ s, D would be of order 1 cm^2/s. Using Einsteins relation, $\mu = \frac{eD}{k_B T}$, where μ is the mobility, e is the electron charge, k_B is the Boltzmann constant and T is the temperature, we conclude that $\mu = 40$ cm^2/V-s would be required. Such large diffusion constants (and mobilities) are not possible either for charged polarons or for neutral excitons in disordered polymers: from picosecond transient photoconductivity measurements the charge carrier (polaron) mobility in semiconducting polymers has been estimated to be[34] 0.5 cm^2/V-s. Under steady state conditions, the carrier mobility is much smaller. $D = 2 \times 10^{-4}$ cm^{2}s^{-1} was estimated for PPV in the ns quenching experiments[20] mentioned above. Neutral exciton diffusion constants are only of order 10^{-5}–10^{-4} cm^{2}s^{-1} even in organic single crystals.[35] Therefore, in order to explain the rapid charge transfer over such long distances, the wavefunctions of the primary excitations must be spatially extended over distances approaching 100 Å.

In the remainder of this section, we present a detailed analysis of the decay which enables a quantitative estimate of the charge transfer range. There has been a considerable volume of recent work[20,36,33,37,38] concerning the nature

of the excited-state species in conjugated polymers, and in particular which species contribute to the near-IR PA band around 800 nm. For simplicity we will assign the PA of pristine MEH-PPV at 800 nm to a single excited-state species. We denote the population of this excited state as N_{ex}. For the following discussion, the size of the exciton binding energy is not important. Moreover, it is not relevant if the primary excitation is emissive or non-emissive.

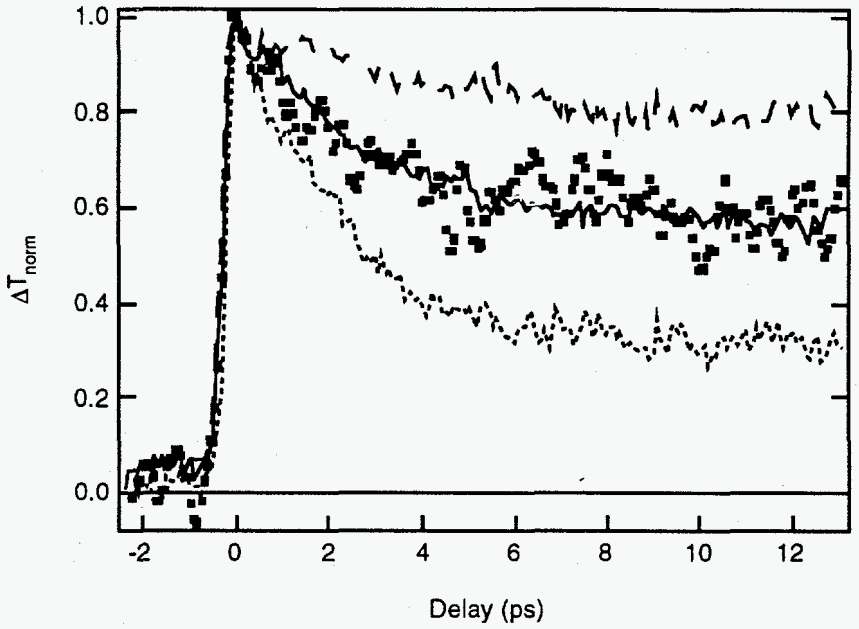

Figure 5. Decay dynamics for MEH-PPV/C_{60} blends: 0%w (dotted line), 5%w (solid line), 25%w (dashed line); (200 Å) MEH-PPV/(400 Å) C_{60} bilayer (squares).

A number of recent papers have discussed bimolecular annihilation processes in PPV derivatives.[33,38–40] It was demonstrated that the intensity-dependent dynamics of the excited state absorption in PPV oligomers can be modeled by a rate equation of the form[33]:

$$\frac{dN_{ex}}{dt} = -\frac{N_{ex}}{\tau} - \frac{\beta}{\sqrt{t}} N_{ex}^2 \tag{7}$$

where the first term represents the natural lifetime decay, and the second term describes the bimolecular decay arising from the interaction between excitations. At low excitation densities, the first term is dominant, and the decay is exponential. At high excitation densities the second term is dominant at early times when the excited species annihilate.[41] The fast initial decay rapidly leads to densities sufficiently low that the natural decay dynamics are recovered at later times.

Bimolecular dynamics of the form shown in Eq. 7 (i.e. with the $t^{-1/2}$ factor) arise in three dimensions (3D) when the interaction between excitations arises from spatial delocalization, rather than from particle diffusion.[41] Particle diffusion in 3D gives a nonlinear component in the rate equation proportional to N_{ex}^2 (independent of time).[41] Since the long-range nature of the charge transfer also implies three-dimensional interactions of the excitons, and since the timescales for the bimolecular decay in our data are again too rapid for diffusion to be important, we use the form as shown in Eq. 7 which accounts only for annihilation by wavefunction overlap in the 3D limit.

The early time decay dynamics for pristine MEH-PPV (the thick sample) are presented in Fig. 6. The parameters used to fit the data are the natural lifetime $\tau = 500$ ps and the bimolecular factor $\beta = 1.2 \times 10^{-20}$ $cm^3 ps^{-1/2}$. As expected, the fast component of the population decay is reduced when the initial excitation density decreases. The quality of the fits implies that Eq. 7 (with the $t^{-1/2}$ factor) can provide a simple quantitative means to understand the intensity-dependent recombination dynamics in these materials, despite the fact that in Eq. 7 many features of decay in real samples are neglected, including nonexponential decay mechanisms at low excitation densities, and also the variation of excitation density along the sample due to absorption of the pump beam. This latter effect in the bilayers results in an excitation density at the rear of the sample approximately 0.6 times the value at the

entrance face; in the bulk samples the variation along the sample is larger still. However, a more detailed model is not necessary to show the basic physical features which contribute to the decay in our samples. In the presence of C_{60}, the excited-state absorption $\Delta\alpha$ arises from a superposition of the remaining primary excitations, N_{ex}, and the newly formed charge-transfer excitations, N_{CT}:

$$\Delta\alpha(t,\lambda) = N_{ex}(t)\sigma_{ex}(\lambda) + N_{CT}(t)\sigma_{CT}(\lambda). \tag{8}$$

The spectral dependence of each excited species is determined by its cross section, $\sigma(\lambda)$.

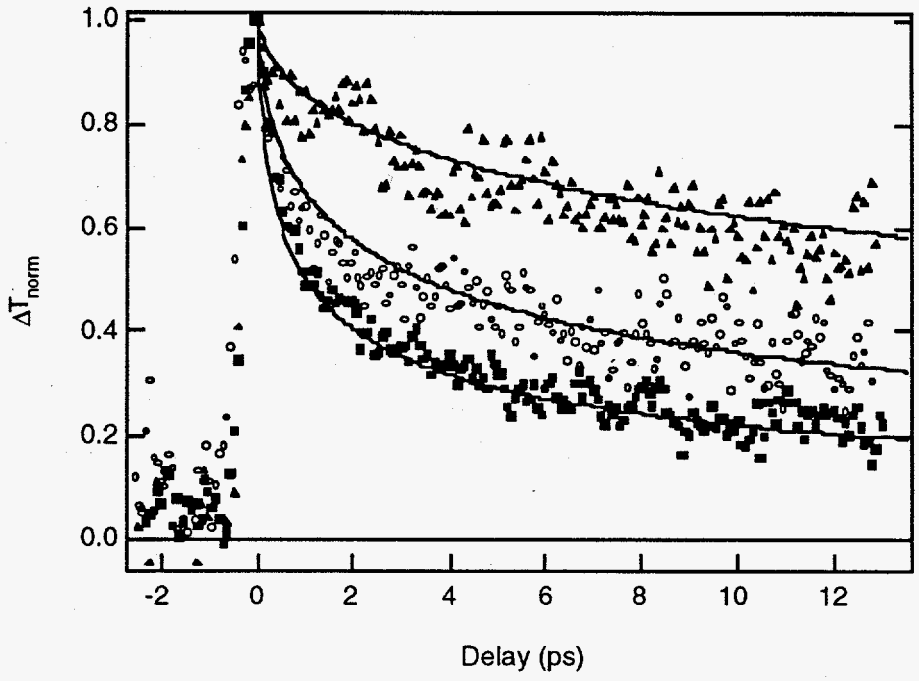

Figure 6. Decay dynamics for 2000 Å MEH-PPV films at various incident excitation densities: $N_0 = 5 \times 10^{19}$ cm^{-3}, squares; $N_0 = 2.5 \times 10^{19}$ cm^{-3}, circles; $N_0 = 5 \times 10^{18}$ cm^{-3}, triangles; the lines represent solutions to a bimolecular decay rate equation (Eq. 7).

The physical model that describes the experimental data follows the functional form of Eq. 8, with the following features:

I: The charge-transferred population N_{CT} is formed at times within the experimental resolution ($\leq$ 200 fs)[15,24]

II: The magnitude of N_{CT} is approximately constant in the picosecond regime.

Eq. 8 implies that the two components of the excited state population are not strongly interacting. Ultrafast creation of a population N_{CT} of charged-transferred states (**I** above) leaves behind a population $N_{ex} = N_0 - N_{CT}$ of primary states on the polymer chains. This reduced "initial" population of N_{ex} then decays via its intrinsic decay channels. **II** is valid because the forward and the reverse charge transfer rates are highly asymmetric; while the forward charge transfer occurs on sub-ps times, the lifetime for the charge transferred state can be up to milliseconds.[1,24] Thus, during the first 10 ps, the contribution of N_{CT} to $\Delta\alpha$ will be approximately constant.

We have shown that for neat MEH-PPV the nonlinear decay of the primary excitations N_{ex} can be deduced from the intensity-dependent decay of $\Delta\alpha$ at 800 nm. In the bilayer, creation of N_{CT} states reduces N_{ex} and hence reduces the bimolecular decay of N_{ex}. In addition, the states N_{CT} contribute a near-constant component to the decay dynamics. The combined effect is a slowing down of the PA decay. In the following, we use parameters derived from the fits of the dynamics in the thin layers of MEH-PPV, together with the relative magnitude of $\Delta\alpha$ at 800

nm in the bilayer, to deduce both the charge transfer probability ξ and the relative excited-state cross section of the charge transferred state, σ_{CT}/σ_{ex}. To do this, we first normalize the measured ΔT/T curve in the bilayer to the value of the pristine thin film at a zero delay, and we rewrite Eq. 8 in the form:

$$\Delta T_{norm} = (1-\xi)\cdot g(t,\xi) + \xi \cdot \frac{\sigma_{CT}}{\sigma_{ex}} \tag{9}$$

The decay function g(t,ξ) in the first term of Eq. 9 is simply the nonlinear decay obtained by integrating Eq. 7 with the same parameters τ and β used to fit the dynamics of the primary excitations N_{ex} in the pristine samples. The dependence of this decay function on ξ is included explicitly to indicate the sensitivity of the bimolecular decay to the percentage of states undergoing charge transfer, as described above. The second term accounts for the time-independent contribution to ΔT/T from N_{CT}; the correct magnitude for this second term is crucial to achieve the proper value of ΔT_{norm} at zero delay (0.82 in our measurement) relative to the pristine thin film. The strength of the two components (found self-consistently) yields the relative fraction of the two species which contribute to the excited state absorption at 800 nm. As shown in Fig. 7, this simple self-consistent model yields excellent fits to the data. The fraction of charge-transferred states extracted from the fit is $\xi = 0.38 \pm .03$, with a value of $\sigma_{CT}/\sigma_{ex} = 0.53 \pm .04$. A corresponding fraction of the polymer layer participates in the charge transfer. Therefore, we infer an effective charge transfer range of approximately 80 Å from the fit in Fig. 7. This more accurate value is consistent with the qualitative conclusion, inferred from the observation that charge-transfer occurs in the picosecond-time scale in bilayer structures (thickness 200 Å), that the charge transfer range is a significant fraction of the film thickness.

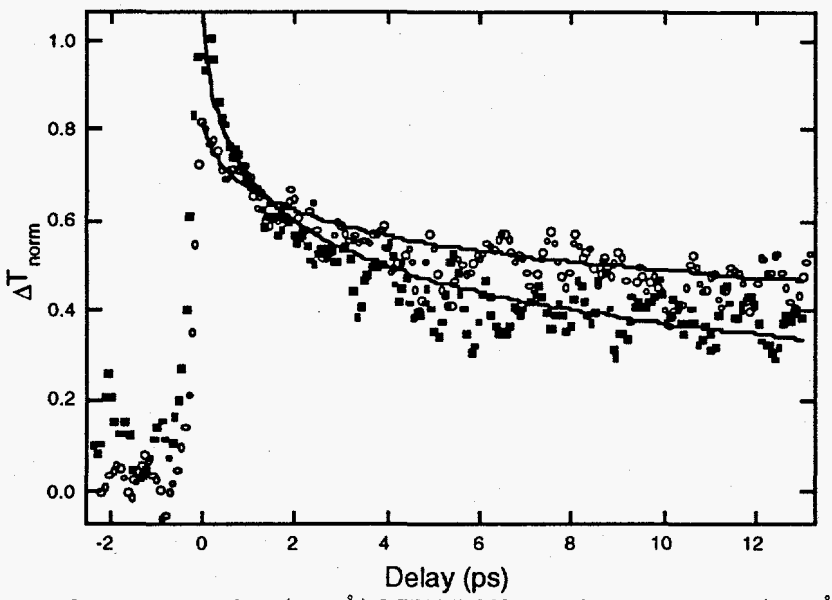

Figure 7. Decay dynamics for thin (200 Å) MEH-PPV monolayer: squares; (200 Å) MEH-PPV/(400 Å) C_{60} bilayer: circles. The lines represent fits to a model involving bimolecular decay of primary excitations in the MEH-PPV and a constant contribution from long-lived charge-transferred states (see text).

We showed in Fig. 5 that the PA dynamics for the bilayer and for the 5%w blend are almost the same, implying a similar fraction of charge-transferred species in these two cases: about 40%. The obvious trend for the MEH-PPV/fullerene blends is that as the concentration of C_{60} increases, a larger fraction of the primary excitation population undergoes charge transfer in the first picosecond. However, even at high concentrations, the efficiency of charge transfer on picosecond timescales does not reach 100%. The high concentration limit was studied by Kraabel et. al.[24] in transient PA measurements of 50%M functionalized fullerene/polymer blends. The data presented in Figure 6 of Reference[24] indicate that even at these high concentrations some decay is observed on the ps timescale; the intrinsic decay of on the order of 15% of the excitations remaining on the polymer accounts for this observed decay, and implies that phase separation of the polymer/fullerene composite at high concentrations of fullerene is the limiting factor for complete charge transfer within the first picosecond. On longer timescales, of course, diffusion still plays a significant role in the charge transfer process, especially for composites at lower fullerene concentrations.

For example, we conclude that in the 5%w bulk blend approximately 40% of the primary excitations undergo charge transfer in the first picosecond. However, the luminescence in these samples is quenched by more than three orders of magnitude, indicating that on timescales intermediate between the intrinsic forward transfer time and the radiative lifetime (10 ps - 1 ns) the diffusion of excitations to find acceptor sites is the dominant decay channel for the remaining excitations on the polymer.

5. CONCLUSIONS

In summary, we have presented results demonstrating charge transfer dynamic grating formation in conducting polymer/C_{60} blends. By comparing the measured response of the TDE with results reported in the literature, it has been demonstrated that this new class of materials exhibits between two and 12 orders of magnitude greater response than any other class of material. In addition, we have presented an analysis which allows comparison of the diffraction efficiency for non-degenerate and degenerate four wave mixing.

The fact that a large fraction of excited states undergo charge transfer in bilayer structures implies that the charge transfer range is a significant fraction of the film thickness. In order to obtain more quantitative results, a model was developed which assumes that the PA dynamics results from two non-interacting species, the primary excitations and the charge-transferred states. Charge transfer occurs in less than a picosecond. The primary excitations follow bimolecular decay dynamics, while the charge-transferred states are longed-lived. Based on this model we conclude that in the bilayers, 38±3% of the initial photoexcitations on the polymer undergo ultrafast charge transfer. A similar fraction of the initial photoexcitations are charge transferred in the 5%w blends. The ratio of excited-state absorption cross-sections of the charge transferred state to the polymer excited state at 800 nm is $\sigma_{CT}/\sigma_{ex} = 0.53 \pm .04$.

Diffusion of localized excitations to the interface cannot explain the observation of charge transfer in bilayers within the picosecond regime; the required diffusion constants for charged polarons or for neutral excitons would be too large by at least two orders of magnitude. In order to explain the rapid charge transfer over such long distances, the wavefunctions of the primary excitations must be spatially extended over approximately 80 Å. The inferred spatial extent of the wavefunction of 80 Å is larger than the value of 30 Å (5 monomers) often quoted for PPV,[42] and would imply spatial delocalization over approximately 13 monomers. The persistence length for MEH-PPV has been estimated[43] to be 60 Å (in solution); this would be a lower bound for delocalized, weakly interacting polarons. McBranch et al showed[44] that for thin films, spin cast at high r.p.m. the polymer chains are arranged primarily parallel to the substrate. In the bilayer structures, the MEH-PPV layer was thin (200 Å) and was spin-cast at 4000 r.p.m. implying that the delocalization length estimated in this work is primarily transverse to the polymer chains. A quasi-3-dimensional wavefunction, extended over 80 Å for the primary excitations of the luminescent polymers is in agreement with the 100 Å localization length found from studies of the metal-insulator transition in conducting polymers (polyaniline and polypyrrole).[45,0] The large spatial spread of the primary excitations inferred from the present measurements implies a weak binding energy of the primary emissive exciton; i.e. 0.05-0.1 eV, or a few times kT.

6. ACKNOWLEDGMENTS

We thank Jun Gao, Christian Heller and Dr. Ian Campbell for assistance with sample preparation. We benefited from discussions with Dr. Ben Schwartz, Kirk Miller Dr. Brett Kraabel and Dr. Uli Lemmer. Work at UCSB was supported by the Air Force Office of Scientific Research (Dr. Charles Lee, Program Officer) under Grant No. F49620-96-1-0107 and by a Los Alamos National Laboratory-University of California program, Grant No. STP/UC:96-136. Work at Los Alamos was also funded through the Laboratory Directed Research and Development Program, under the auspices of the U.S. Department of Energy.

REFERENCES

1. N. S. Sariciftci, L. Smilowitz, A. J. Heeger, and F. Wudl, "Photoinduced electron transfer from a conducting polymer to buckminsterfullerene," *Science* **258**, p. 1474, 1992.
2. G. Yu, J. Gao, J. Hummelen, F. Wudl, and A. Heeger, "Polymer photovoltaic cells: enhanced efficiencies via a network of internal donor-acceptor heterojunctions," *Science* **270**, pp. 1789–1791, 1995.
3. E. Maniloff, D. Vacar, D. McBranch, H. Wang, B. Mattes, J. Gao, and A. Heeger *Opt. Comm., in press* , 1997.

4. M. Cha, N. S. Sariciftci, A. J. Heeger, J. C. Hummelen, and F. Wudl, "Enhanced nonlinear absorption and optical limiting in semiconducting polymer/methanofullerene charge-transfer films," *Appl. Phys. Lett.* **67**, p. 3850, 1995.
5. D. Vacar, E. Maniloff, D. McBranch, and A. Heeger, "Charge transfer range for photoexcitations in conjugated polymer/fullerene blends," *Phys. Rev. B* **56**, p. in press, 1997.
6. P. Gunter and J.-P. Huignard, *Photorefractive Materials and Their Applications*, Springer-Verlag, NY, 1988.
7. E. S. Maniloff and K. M. Johnson, "Maximized photorefractive holographic storage," *J. Appl. Phys.* **70**, pp. 4702 – 4707, 1991.
8. H. Eichler, P. Gunter, and D. Pohl, *Laser-Induced Dynamic Gratings*, Springer-Verlag, NY, 1986.
9. W. E. Moerner and S. M. Silence, "Polymeric photorefractive materials," *Chem. Revs.* **94**, p. 127, 1994.
10. J. Xu, G. Zhang, Q. Wu, Y. Liang, S. Liu, Q. Sun, X. Chen, and Y. Shen, "Holographic recording and light amplification in doped polymer film," *Opt. Lett.* **20**, pp. 504–506, 1995.
11. C. Halvorsen, A. Hays, B. Kraabel, R. Wu, F. Wudl, and A. J. Heeger, "A 160-femtosecond optical image processor based ona conjugated polymer," *Science* **265**, pp. 1215–1216, 1994.
12. B. Volodin, Sandalphon, K. Meerholz, B. Kippelen, N. Kukhtarev, and N. Peygambarian, "Highly efficient photorefractive polymer for dynamic holography," *Opt. Eng.* **34**, pp. 2213 – 2223, 1995.
13. P. Yeh, A. Chiou, and J. Hong, "Optical interconnections using photorefractive dynamic holograms," *Appl. Opt.* **27**, p. 2093, 1988.
14. N. S. Sariciftci and A. J. Heeger *Int. J. Mod. Phys. B* **8**, p. 8237, 1994.
15. B. Kraabel, D. McBranch, N. S. Sariciftci, D. Moses, and A. J. Heeger, "Ultrafast spectroscopic studies of photoinduced electron transfer from semiconducting polymers to c_{60}," *Phys. Rev. B* **50**, p. 18543, 1994.
16. K. Lee, E. K. Miller, N. S. Sariciftci, J. C. Hummelen, F. Wudl, and A. J. Heeger, "Photoinduced absorption and photoinduced reflectance in conducting polymer/methanofullerene films: nonlinear optical changes in the complex refractive index," *Phys. Rev. B* **54**, pp. 10525–10529, 1996.
17. J. Brèdas, J. Cornil, and A. Heeger, "The exciton binding energy in luminescent conjugated polymers," *Adv. Mater.* **8**, p. 447, 1996.
18. J. Leng, S. Jeglinski, X. Wei, R. Benner, and Z. Vardeny *Phys. Rev. Letts* **72**, pp. 156 – 159, 1994.
19. M. Chandross, S. Mazumdar, M. Liess, P. Lane, Z. Vardeny, M. Hamaguchi, and K. Yoshino, "Optical absorption in the substituted phenylene-based polymers: theory and experiment," *Phys. Rev. B* **55**, p. 1486, 1997.
20. L. Rothberg, F. Papadimitrakopoulos, and M. Galvin, "Photophysics of phenylenevinylene polymers," *Synthetic Metals* **80**, pp. 41–58, 1996.
21. J. Halls, K. Pichler, R. Friend, S. Moratti, and A. Holmes, "Exciton diffusion and dissociation in a poly(*p*-phenylene vinylene)/c_{60} heterojunction," *Appl. Phys. Lett.* **68**, pp. 3120–3122, 1996.
22. V. Choong, Y. Park, Y. Gao, T. Wehrmeister, K. Mullen, B. Hsieh, and C. Tang, "Dramatic photoluminescence quenching of phenylene vinylene oligomer thin films upon submonolayer ca deposition," *Appl. Phys. Lett.* **69**, pp. 1492–1494, 1996.
23. N. Harrison, G. Hayes, R. Phillips, and R. Friend, "Singlet intrachain exciton generation and decay in poly(p-phenylenevinylene)," *Phys. Rev. Lett.* **77**, pp. 1881–1884, 1996.
24. B. Kraabel, J. Hummelen, D. Vacar, D. Moses, N. S. Sariciftci, A. J. Heeger, and F. Wudl, "Subpicosecond photoinduced electron transfer from conjugated polymers to functionalized fullerenes," *J. Chem. Phys.* **104**, pp. 4267–4273, 1996.
25. X. Wei, S. Frolov, and Z. Vardeny, "Studies of photoexcitations in conducting polymers mixed with c_{60}," *Synth. Met.* **78**, pp. 295–299, 1996.
26. V. Pham, G. Manivannan, R. Lessard, and R. Po *Opt. Mat.* **4**, pp. 467–475, 1995.
27. J. Zhao, F. Dong, H. Qu, P. Ye, X. Fu, L. Qiu, and Y. Shen, "Dynamic studies on laser-induced gratings in azobenzene-doped polymer film," *Appl. Phys. B* **61**, pp. 377–384, 1995.
28. P. Wu, W. Chen, X. Gong, G. Zhang, and G. Tang, "Red band holographic storage in azo dye sensitized by noncoherent light," *Opt. Lett.* **21**, pp. 429 – 431, 1996.
29. R. Tarkka, M. Talbot, D. Brady, and G. Schuster, "Holographic storage in a near-ir sensitive photochromic dye," *Opt. Comm.* **109**, pp. 54 – 58, 1994.

30. P. Foote, G. Proudley, G. Beddard, G. McFadyen, G. Reid, L. Connors, M. Bell, T. Hall, and K. Powell, "Picosecond optical correlation using dynamic holography on polyacetylene," *Appl. Opt.* **32**, pp. 174 – 178, 1993.
31. Y. Pang and P. N. Prasad *J. Chem. Phys.* **92**, p. 2201, 1990.
32. P. N. Prasad and D. J. Williams, *Introduction to Nonlinear Optical Effects in Molecules and Polymers*, Wiley-Interscience, NY, 1991.
33. E. Maniloff, V. Klimov, and D. McBranch, "Intensity-dependent relaxation dynamics and the nature of the excited-state species in solid-state conducting polymers," *Phys. Rev. B* **56**, pp. 1876–1881, 1997.
34. C. Lee, G. Yu, D. Moses, and A. J. Heeger, "Picosecond transient photoconductivity in poly(*p*-phenylene vinylene)," *Phys. Rev. B* **49**, pp. 2396–2407, 1994.
35. M. Pope and C. Swenberg, *Electronic processes in organic crystals*, Clarendon Press, Oxford, 1982.
36. B. Schwartz, F. Hide, M. Andersson, and A. Heeger, "Ultrafast studies of stimulated-emission and gain in solid films of conjugated polymers," *Chem. Phys. Lett.* **265**, pp. 327–333, 1997.
37. D. McBranch and M. Sinclair in *The Nature of the Photoexcitations in Conjugated Polymers*, N. Sariciftci, ed., World Scientific Publishing, Singapore, 1997.
38. V. Klimov, D. McBranch, N. Barashkov, and J. Ferraris, "Femtosecond dynamics of excitons in π-conjugated oligomers: the role of intrachain two-exciton states in the formation of interchain species," *Chem. Phys. Lett., in press* , 1997.
39. R. Kepler, V. Valencia, S. Jacobs, and J. McNamara, "Exciton-exciton annihilation in poly(p-phenylenevinylene) films," *Synthetic Metals* **78**, pp. 227–230, 1996.
40. G. Denton, N. Harrison, N. Tessler, and R. Friend, "Factors influencing stimulated-emission from poly(p-phenylenevinylene)," *Phys. Rev. Lett.* **78**, pp. 733–736, 1997.
41. R. Powell and Z. Soos, "Singlet exciton energy transfer in organic solids," *J. Luminescence* **11**, pp. 1 – 45, 1975.
42. D. Beljonne, Z. Shuai, R. Friend, and J. Bredas, "Theoretical investigation of the lowest singlet and triplet states in poly(*para*-phenylene vinylene oligomers," *J. Chem. Phys.* **102**, pp. 2042–2049, 1995.
43. C. Gettinger, A. Heeger, J. Drake, and D. Pine, "A photoluminescence study of ploy(*p*-phenylene vinylene derivatives: the effect of intrinsic persistence length," *J. Chem. Phys.* **101**, pp. 1673–1678, 1994.
44. D. McBranch, I. Campbell, D. Smith, and J. Ferraris, "Optical determination of chain orientation in electroluminescent polymer films," *Appl. Phys. Lett.* **66**, pp. 1175–1177, 1995.
45. M. Reghu, Y. Cao, D. Moses, and A. J. Heeger, "Counterion-induced processibility of polyaniline: transport at the metal-insulator boundary," *Phys. Rev. B* **47**, pp. 1758–1764, 1993.
46. C. Yoon, M. Reghu, D. Moses, and A. J. Heeger, "Transport near the metal-insulator transition: polypyrrole doped with PF(6)," *Phys. Rev. B* **49**, pp. 10851–10863, 1994.